Environmental Technology

ISSN: (Print) (Online) Journal homepage: www.tandfonline.com/journals/tent20

Two-stage leaching of calcium and vanadium from high-calcium steelmaking slag

Maria Kokko, Toni Kauppinen, Tao Hu, Pekka Tanskanen, Rita Kallio, Ulla Lassi & Janne Pesonen

To cite this article: Maria Kokko, Toni Kauppinen, Tao Hu, Pekka Tanskanen, Rita Kallio, Ulla Lassi & Janne Pesonen (13 Feb 2024): Two-stage leaching of calcium and vanadium from high-calcium steelmaking slag, Environmental Technology, DOI: 10.1080/09593330.2024.2316671

To link to this article: https://doi.org/10.1080/09593330.2024.2316671

ENVIRONMENTAL TECHNOLOGY
https://doi.org/10.1080/09593330.2024.2316671

Two-stage leaching of calcium and vanadium from high-calcium steelmaking slag

Maria Kokko[a], Toni Kauppinen[a,b], Tao Hu[a], Pekka Tanskanen[c], Rita Kallio[c], Ulla Lassi[a,b] and Janne Pesonen [a]

[a]Research Unit of Sustainable Chemistry, University of Oulu, Oulu, Finland; [b]Kokkola University Consortium Chydenius, University of Jyväskylä, Kokkola, Finland; [c]Research Unit of Process Metallurgy, University of Oulu, Oulu, Finland

ABSTRACT

Vanadium (V) is a critically important element in many industries. A widely used recovery process is a combination of roasting and leaching. However, roasting is an energy-intensive stage. Generally, basic oxygen furnace (BOF) slag is high in calcium (Ca) but low in V. Ca content and its chemical nature can prevent V leaching. This study presents a potential two-stage leaching process for Ca and V from BOF slag. The method is environmentally friendly using low temperatures and enabling leachate recycling. Furthermore, the utilisation rate of the slag can be higher due to Ca recovery. Ca is first leached using ammonium nitrate and nitric acid solution. The V-containing residue is directed to the second stage, where V is leached using ammonium carbonate ($(NH_4)_2CO_3$). Ca leaching efficiency was 71% achieved with a low temperature (40°C) and in 20 min. > 99% of the dissolved element was Ca. Increasing the total nitrate concentration increased the leaching efficiency. Reducing the L/S ratio improved selectivity. The solid material was analysed after the leaching stages and a clear change was observed after the Ca-stage. The V leaching efficiency was 50%. > 88% of dissolved element was V (L/S 8, [$(NH_4)_2CO_3$] 200 g/L, 60°C, and 60 min). Increasing [$(NH_4)_2CO_3$] and L/S ratio slightly improved the leaching efficiency but decreased selectivity. The studied process implements circular economy principles and has been developed for side streams with low V concentrations. However, further optimisation and developments are required regarding the effectiveness of the process.

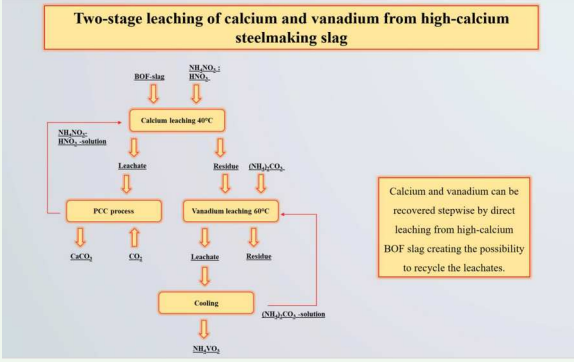

ARTICLE HISTORY
Received 18 October 2023
Accepted 29 January 2024

KEYWORDS
Vanadium; calcium; direct leaching; BOF slag; hydrometallurgy

1. Introduction

The European Commission has listed vanadium (V) as one of the critical raw materials for the European Union [1]. It is used in several industries, such as the chemical, ceramic, steel, and battery industries. V is a more common element in the Earth's crust than copper or nickel, but it is widespread in the Earth's crust, so it does not occur as concentrated deposits [2]. However, V content can be significant in secondary raw materials, such as steelmaking slags, and their utilisation as a source of V has been studied.

The V recovery has been studied by direct pressured leaching [3,4]. However, a more common procedure includes a combination of roasting and leaching before ammonium precipitation [5,6]. Roasting oxidises low-valence V species to higher oxidation states and decomposes the stable iron phases, transforming V into a more soluble form [7]. However, a non-salt

CONTACT Janne Pesonen janne.pesonen@oulu.fi Research Unit of Sustainable Chemistry, University of Oulu, PO Box 4300, FI-90570 Oulu, Finland
Supplemental data for this article can be accessed online at https://doi.org/10.1080/09593330.2024.2316671.

roasting [7–10] and a roasting with sodium (Na) or Ca salt addition [8,11–15] requires high temperatures and polluting gases are emitted during alkaline roasting (e.g. Na_2CO_3, Na_2SO_4, NaCl) [16,17].

Water [16,18], alkaline [9,14], or acid [11,12,19] is commonly used as a leaching agent, but the main problem is non-selective leaching. Silicon (Si), phosphorus (P), and chromium (Cr) are often the main impurities in water and alkali leaching [9,16,20,21]. Due to the high concentrations of impurities, purification is often complicated [22]. In many of the proposed processes, the leachate cannot be recycled. In acidic leaching consumption of reagents is high due to the high lime content in steel slags [22]. Furthermore, Si concentration is significant [23–26]. The dissolution of silica and the formation of silica gel [27] can become a challenge in the recovery of V. Dissolved vanadate is precipitated by adding ammonium salt (e.g. ammonium sulfate, ammonium chloride) to the purified leachate at a suitable pH [18,20,28,29] and temperature [8,20].

Some studies have investigated the recovery of V by direct leaching from high Ca content steel slag [17]. Ca is divided into several phases in BOF slag [30] and from some of those it can dissolve fairly easily. Due to its high concentration and chemical nature, Ca can become a problem in V recovery. However, Ca can be bound to the solid as sulfate, hydroxide, or carbonate, but this consumes a lot of reagents. This also increases the amount of produced solid waste. Therefore, Ca recovery before V leaching is desirable. After selective Ca leaching, it can be utilised as calcium carbonate. This increases the utilisation rate of the slag. This study presents a Ca and V recovery method where Ca can be utilised as calcium carbonate and V as ammonium vanadate.

The aim of this study was to develop an environmentally friendly direct leaching of Ca and V from the BOF slag. The leaching was done in two stages. In the first stage, Ca is dissolved in an ammonium nitrate and nitric acid (NH_4NO_3-HNO_3) solution. The V-containing residue is directed to the second stage, where V is leached with $(NH_4)_2CO_3$. This process follows the principles of circular economy and to our knowledge, a fully hydrometallurgical method of Ca extraction followed by V leaching from high-Ca BOF slag has not been previously studied.

2. Materials and methods

2.1. Raw material and reagents

The BOF slag utilized in these experiments was sourced from a steel mill in northern Finland. The slag was ground (12.5 microns, D50) and used in the Ca leaching stage. The residue from the first stage was directed to the V leaching stage. In the leaching experiments, HNO_3 > 69% (Honeywell, USA, puriss. p.a.), NH_4NO_3, (VWR Chemicals BDH, USA, 99.5%), and ammonium carbonate ($(NH_4)_2CO_3$, Thermo Scientific, USA, extra pure) were used as the reagents. In addition to nitric acid, hydrofluoric acid (HF; 40%; VWR Chemicals BDH, USA), hydrochloric acid (HCl; 37%; Fisher Chemical), and boric acid were used in acid digestion.

2.2. Experimental design of leaching

Ammonium salt solutions (NH_4Cl, NH_4NO_3, CH_3COONH_4) have been proposed as selective extraction solutions for Ca [31]. However, the leaching efficiency remains lower than when using strong acids. HNO_3 has been studied for its potential to dissolve Ca almost completely, but the selectivity of the leaching process is poor [25,31]. In this study, to maximise the Ca leaching efficiency and prevent the V leaching a solution of NH_4NO_3 and HNO_3 (ratio 3:1) was used in the Ca-stage. The experiments with temperatures of 25°C and 40°C were performed in a beaker and with 70°C in a 250 mL three-neck round-bottom flask. A reflux condenser and plastic caps were used to prevent excessive evaporation of the liquid. The stirring speed was maintained at 350 rpm. The solution was heated to the desired temperature before the addition of the slag. The reaction time started with the addition of the slag. Leaching was followed by filtration, and the residue was washed with deionised water. Investigated reaction conditions in the Ca-stage are shown in Table 1.

The V-containing residue was directed to the second stage and V leaching was performed by using $(NH_4)_2CO_3$. The experiments were performed in a three-neck round-bottom flask tightly closed with rubber and glass caps. The stirring speed was maintained at 280–290 rpm. When using lower (≤200 g/L) concentrations, the ammonium carbonate solutions were prepared in a volumetric flask. With higher $(NH_4)_2CO_3$ concentrations (≥300 g/L), solid $(NH_4)_2CO_3$ was weighed straight into a three-neck round-bottom flask. The reaction time started with the addition of reagents and residue. Washing after filtration was carried out using warm

Table 1. Optimised parameters in the Ca leaching stage.

Parameter(s) to be investigated	Time (min)	$[NO_3^-]$ (mol/L)	L/S (mL/g)	Temp. (°C)
$[NO_3^-]$ with different L/S ratios	20	5, 6, 7	5, 8, 10	40
Temperature	20	7	5	20, 40, 70

Table 2. Investigated parameters in the V leaching stage.

Parameter(s) to be investigated	Temp. (°C)	Time (min)	$[(NH_4)_2CO_3]$ (g/L)	L/S (mL/g)
Reaction time and temperature	60, 70, 80, 90	60, 120	100	8
L/S ratio	60	60	100	8, 12, 16
Concentration	60	60	100, 200, 300, 400, 500, 600	8

deionised water to prevent untimely crystallization of ammonium vanadate. The studied parameters are shown in Table 2.

2.3. Characterization methods

The solid samples were digested by microwave-assisted acid digestion to determine the elemental concentrations of the solid material. The digestion was done by Rantala et. al validated method 2 [32]. Measurements were performed using inductively coupled plasma–optical emission spectroscopy (ICP–OES, Agilent 5110). X-ray diffraction analysis (PANalytical X'Pert Pro, CuKα_1 radiation, 40 mA, 45 kV, 2θ values from 10° to 70°) was used to identify the phases of the original slag and the residues. Electron probe microanalyzer–wavelength-dispersive spectroscopy (EPMA–WDS JEOL JXA-8530FPlus) results were used to identify the chemical composition of the phases. Modal mineralogy was studied by field emission scanning microscope-energy dispersive spectroscopy (FESEM-EDS JEOL JSM-7900F). Differential scanning calorimetry-thermogravimetry (DSC-TG Netzsch STA449F3) analysis combined with mass spectrometry (MS Netzsch QMS403) was used to confirm some phases in V leaching residue. The concentrations of V, Ca, and impurities (iron (Fe), aluminum (Al), magnesium (Mg), manganese (Mn), and silicon (Si)) in the leachates were determined by ICP–OES (Agilent 5110). The solid samples from the optimised conditions were decomposed as previously described and analysed via ICP–OES to ensure there were suitable concentrations of the main elements in the residues.

The leaching efficiencies (X) of V, Ca, and impurities were calculated according to Equation 1.

$$X = \frac{C_d V_{init.}}{m_0} * 100\%, \quad (1)$$

where C_d is the concentration (mg/L) of the desired element in the leachate, $V_{init.}$ (L) is the initial volume of the solution, and m_0 is the amount (mg) of the investigated element in the slag.

Leachate recycling is possible if the leaching is sufficiently selective towards the desired element. In this study, the method's selectivity was evaluated by calculating the mass fractions of the dissolved elements in the leachates. Element distribution (ED) was calculated using Equation 2.

$$ED = \sum \frac{m_i}{m_{tot}} * 100\%, \quad (2)$$

where ED represents the element distribution of the leachate (%), m_i represents the mass (g) of the desired element in the leachate, and m_{tot} represents the sum of masses (g) of all investigated elements leached to the leachate.

3. Results and discussion

3.1. Mineralogy and elemental distributions of BOF slag

The concentrations of V, Ca, and the main impurities of the BOF slag are shown in Table 3, the chemical composition of the main phases in Table 4, and the results of the mineralogical analysis in Figure 1.

According to the XRD analysis (Figure 1), the Ca-bearing phases and compounds in the slag were calcium hydroxide ($Ca(OH)_2$), lime (CaO), calcium carbonate ($CaCO_3$), calcium ferrite (an intermediate calciumaluminoferrite composition from srebrodolskite and brownmillerite solid solution, interpreted as brownmillerite in Figure 1), and calcium silicate phases (hatrurite and larnite). Quartz could be identified from the XRD result, which is due to the slag handling procedures at the steel plant. EPMA-WDS analysis (Table 4) revealed that the V-containing phases in the slag are calcium vanadate (CV), larnite, and calcium ferrite. Larnite also contained some phosphorus (P), and Fe, most probably replacing Si in the crystal lattice. Lime had increased Fe and Mn contents, and wüstite had typically increased Mg, Mn, and Fe contents. In addition to V, calcium ferrite contained some titanium (Ti), and chromium (Cr) as additional components. CV was a Si-containing variety with increased contents of P and Cr. Lime, wüstite, and hatrurite were low in V contents.

To find out the more precise distribution of V between the different phases, FESEM-EDS modal

Table 3. Elemental concentrations (mg/g) of slag, as measured using ICP–OES analysis.

Concentration of elements (mg/g)	Al	Ca	Fe	Mg	Mn	Si	V	Ti	P
BOF slag	7.43	330.78	151.03	9.92	19.49	51.08	21.81	5.99	3.61

Table 4. Chemical composition of the main phases, as determined via EPMA–WDS analysis (n = number of point analyses).

Phase	n	MgO	Al_2O_3	SiO_2	P_2O_5	Cr_2O_3	CaO	TiO_2	FeO	MnO	V_2O_3	Total
Larnite	27	0.02	0.79	25.92	2.36	0.16	61.82	0.60	1.86	0.20	3.92	97.76
Lime	30	0.89	0.10	0.75	0.09	0.08	83.13	0.08	7.95	4.54	0.29	97.90
Ferrite	22	0.53	5.19	0.55	0.07	2.14	42.65	2.83	35.18	0.90	3.58	93.63
Wüstite	14	11.33	0.00	0.00	0.01	0.16	6.10	0.03	65.72	14.05	0.18	97.59
Hatrurite	8	0.33	0.48	22.81	1.17	0.04	69.08	0.28	2.21	0.93	0.77	98.13
Ca vanadate	10	0.00	0.07	10.89	3.75	2.48	53.07	0.62	0.68	0.06	24.60	96.24

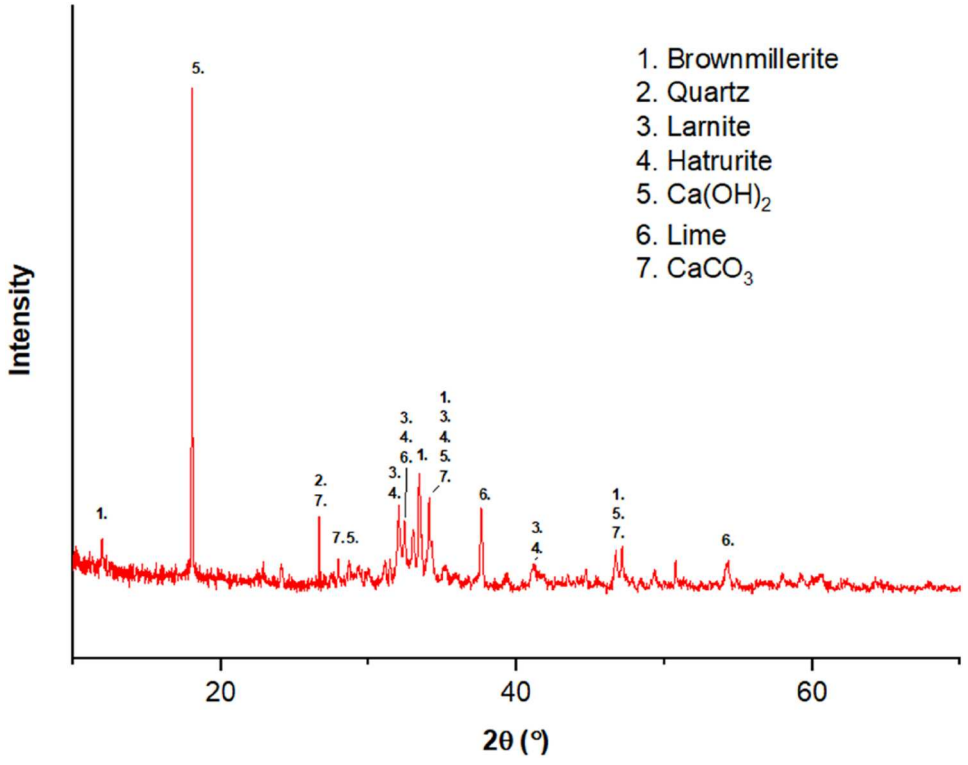

Figure 1. XRD analysis of original BOF slag.

analysis was performed (supplementary data (SD), Figure 1). Based on combined information from modal mineralogy and mineral chemical compositions, most of the V was incorporated in larnite (about 47%) and calcium ferrite (about 32%) and almost 19% in CV with only minor deportment in hatrurite. In the Ca-, and Fe-containing phases V can occur as a trivalent V [30], implicating that the V dissolution might be less favourable [33].

3.2. Calcium leaching

The slag contained approximately 33 wt% Ca, and due to the chemical nature and high concentration of Ca, removing it from the slag was beneficial for the recovery of V. Furthermore, Ca recovery could significantly increase the utilisation of steel production's side streams. The potential for utilising CO_2 to produce precipitated calcium carbonate (PCC) from steel slag has been studied [34] requiring selective leaching of Ca.

Based on preliminary tests, the pH value of the aqueous slag solution was 13.06 after a six-hour shaking test (L/S 10, room temperature). A strong acid is required to neutralise the alkalinity of the slag. H_2SO_4-$(NH_4)_2SO_4$ solution is not suitable due to the goal of Ca utilisation hence NH_4NO_3-HNO_3 solution is presented as the leaching solution. During the Ca-stage, it is essential to prevent the loss of V. Dissolved pentavalent V occurs in the solution as different vanadate species (meta-, pyro-, ortho-, or polyvanadate) or hydrated pentavalent forms depending on the reaction conditions (pH, [V] in the solution) [35]. In the NH_4^+-containing solution with favourable conditions (pH, [V], and temperature) vanadate ions precipitate as ammonium vanadate [35] (Equation 3), thus V is not lost in the Ca-stage. The leachate from the selective Ca-leaching stage can be recycled back to the leaching process

mainly by adjusting the pH. It can be adjusted with HNO_3, preventing the accumulation of ammonium ions in the leachate during recycling. As shown in section 3.1, Ca is mainly located in silicate phases, lime, and Ca (OH)2. The leaching of Ca is represented by reaction Equations 4–6.

$$VO_3^- (aq) + NH_4^+ (aq) \rightarrow NH_4VO_3 (s) \quad (3)$$

$$Ca(OH)_2 (s) + NH_4NO_3 (aq) + HNO_3(aq) \rightarrow Ca(NO_3)_2(aq) + NH_3 (aq) + 2H_2O (l) \quad (4)$$

$$CaO (s) + NH_4NO_3 (aq) + HNO_3(aq) \rightarrow Ca(NO_3)_2(aq) + NH_3 (aq) + H_2O (l) \quad (5)$$

$$Ca_2SiO_4 (s) + 2NH_4NO_3 (aq) + 2HNO_3(aq) \rightarrow 2Ca(NO_3)_2 (aq) + 2NH_3 (aq) + 2H_2O (l) + SiO_2 (s) \quad (6)$$

In this study, Ca leaching was studied with NH_4NO_3 and HNO_3 solution, keeping the ratio of ammonium salt and acid constant (3:1). For simplicity, the concentration is presented as total nitrate concentration [NO_3^-]. Based on the preliminary experiments with [NO_3^-] of 6 and 7 mol/L, Ca dissolved more at a higher [NO_3^-], but V was found to dissolve more at a lower [NH_4^+] (Figure 2). In addition, Ca leaching seemed to be a rapid reaction. Most of the Ca was dissolved in the first five minutes and it seemed to remain unchanged up to 60 min. It can be assumed that Ca has leached from more easily soluble phases under prevailing conditions. Similar results have been found in the literature. Dissolution of Ca has shown to be rapid with acetic acid (CH_3COOH) [36], ammonium chloride (NH_4Cl) [37], and NH_4NO_3 [34] solutions. The temperature data in Figure 2 indicated that the Ca leaching from these phases was an exothermic reaction. The temperature seemed to stabilise close to the initial temperature in 60 min. Based on the preliminary results, the reaction time was set at 20 min.

3.3. Effects of concentration, L/S ratio and temperature

The effect of the L/S ratio and concentration on Ca leaching efficiency (average with relative error bar) and element distribution in the leachate was investigated (Figure 3(a,b)). The pH of the solution changed due to variations in the concentration and L/S ratio and it can be seen from Figure 3(a).

Figure 3(a) shows that the highest and lowest L/S ratio [NO_3^-] of 5 mol/L has a moderately large

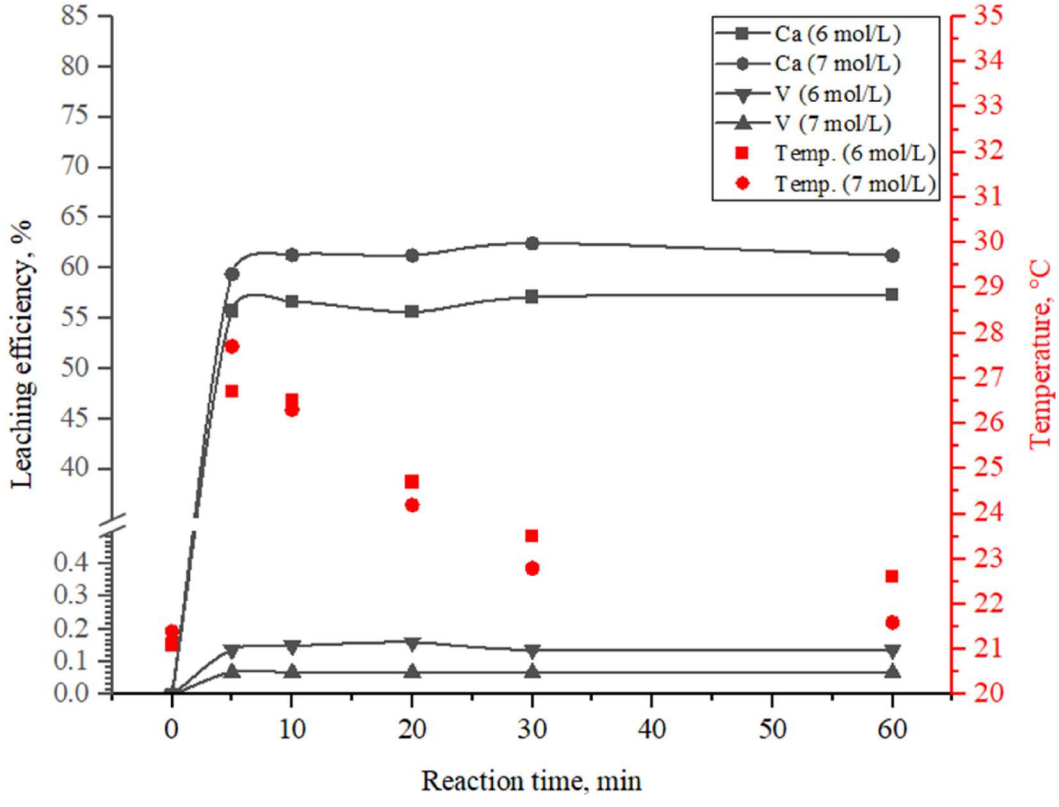

Figure 2. Ca leaching at room temperature with an L/S ratio of 5.

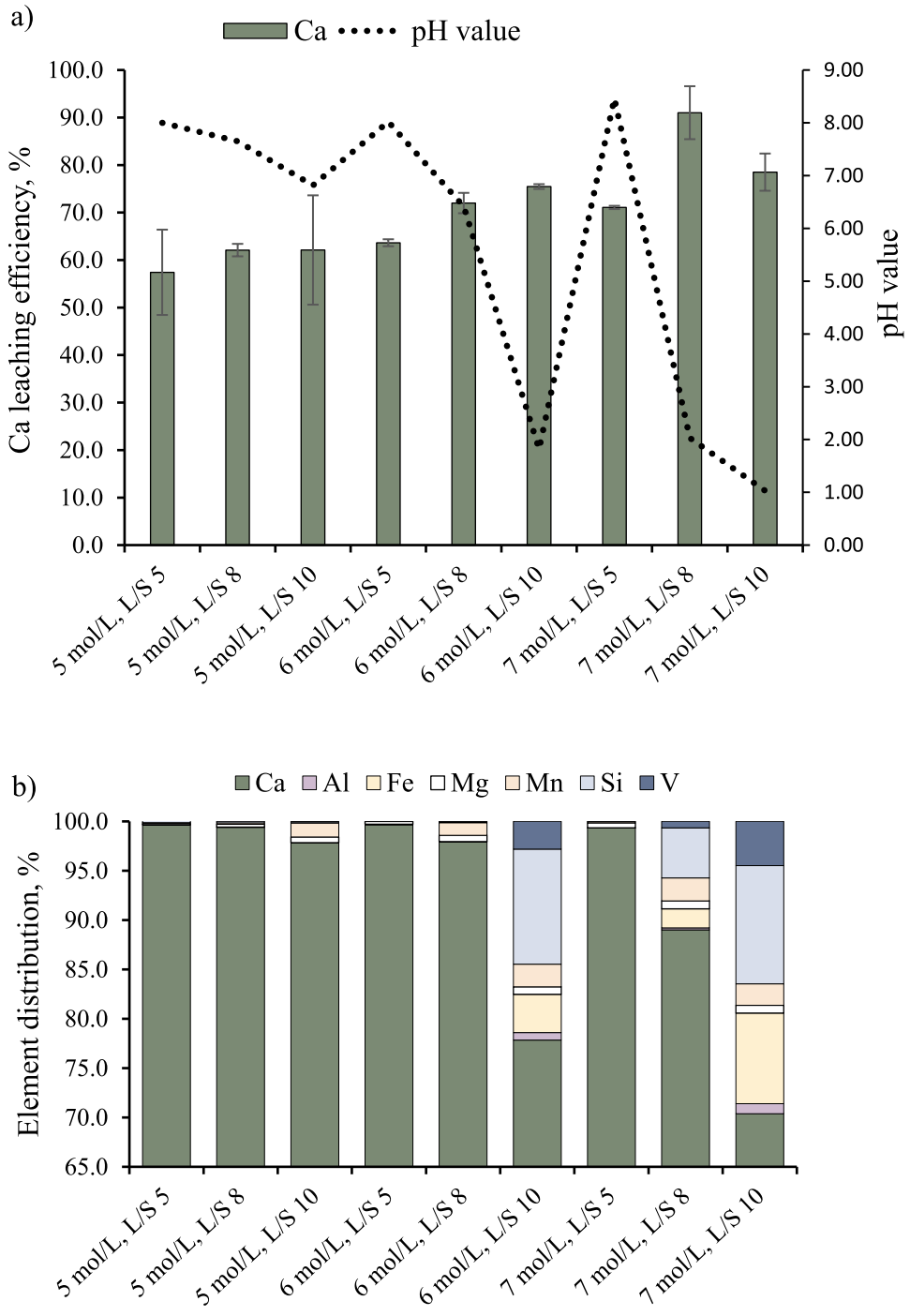

Figure 3. Effects of the different [NO_3^-] and L/S ratios on the (a) Ca leaching efficiency and (b) ED in the leachate (40°C, 20 min).

difference between replicates. This may be due to the relatively small sample portion and heterogeneity of the material. Based on the results, however, it seems that increasing both parameters increases the leaching efficiency of Ca. Eloneva et al. (2008, 2012) investigated Ca leaching efficiency affected by [NH_4NO_3] (from 0 mol/L to 2 mol/L) [31] and L/S ratio (variation between 1.7–50 mL/g) [34]. Their findings support the results of this study. The dramatic decrease in leaching efficiency between L/S 8 and L/S 10 (7 mol/L) might be due to the low pH (<1) and dissolution of silica. At a low pH (<2), dissolved silica can begin to form colloidal silicic acid [38,39], trapping Ca within it [39].

With the lowest [NO_3^-], the proportions of impurities did not significantly increase, even though the L/S ratio increased (Figure 3(b)). At higher [NO_3^-], increasing the L/S ratio increased the relative proportion of

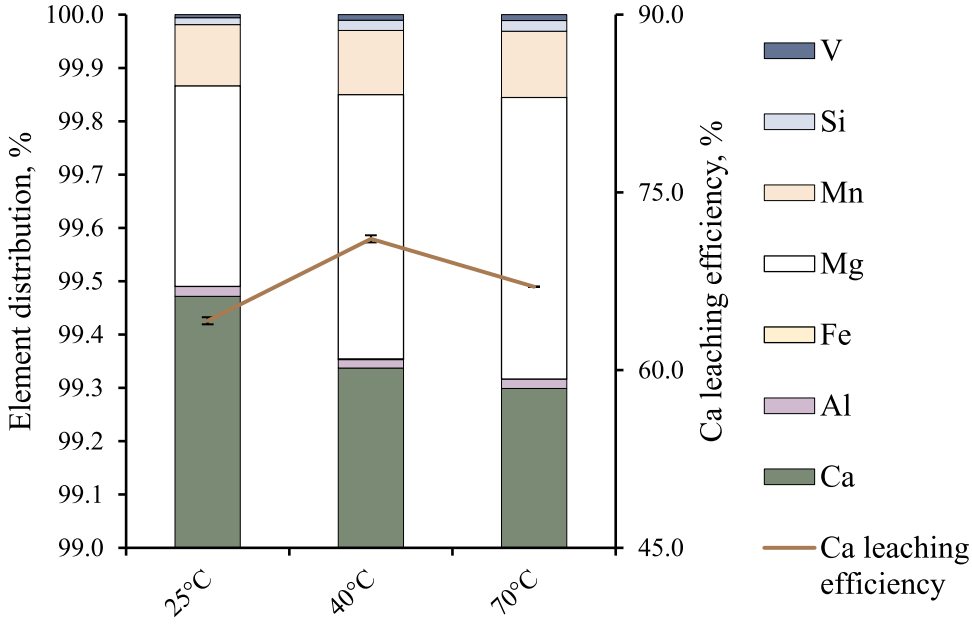

Figure 4. Effect of the temperature on the leaching efficiency of Ca (7 mol/L, L/S 5, 20 min) and ED of leachate.

impurities such as Fe and Si in the leachate. The measured concentrations of the elements shown in Figure 3(b) are presented in SD, Table 1. Furthermore, V concentration increased in the solutions with low pH. If $[H^+]$ is high, the bond between vanadate and ammonium may be broken down. In a sufficiently acidic solution, ammonium vanadate decomposes [40] and releases V into the leachate. It can be inferred from the results that dissolved V is converted to ammonium vanadate at low temperatures [8,15] and a sufficiently high pH.

Precipitation of $CaCO_3$ through the PCC process requires alkaline leachate [37]. The pH of the leachate should be above 8 to avoid the addition of large amounts of reagents. In addition, the purity of the solution should be high, to ensure the quality of the final product. For those reasons, the parameters chosen were L/S ratio 5 and $[NO_3^-]$ 7 mol/L.

The effect of the leaching temperature (25°C, 40°C, and 70°C) was investigated, and Figure 4 illustrates its effect on the leaching efficiency (average with relative error bar) and ED in the leachate. Measured concentrations are presented in SD, Table 2.

Increasing the temperature from 25 to 40 °C increased the leaching efficiency of Ca. However, when the system was heated to 70 °C, the leaching efficiency declined. The temperature had no significant effect on the amount of impurities in the solution. Considering the energy consumption, preventing ammonium evaporation, leaching efficiency of Ca, the purity of the solution, and minimising V loss, the optimal leaching temperature is 40°C (L/S 5, 7 mol/L, 20 min).

3.4. Characterization of Ca leaching residue

The conditions of the Ca-stage were optimised and the concentrations of the elements in the residue were analysed via microwave-assisted acid digestion and ICP–OES measurements (Table 5). The phase composition of the residue was analysed by XRD (Figure 5) and EPMA–WDS (Table 6).

It can be seen from Tables 3 and 5 that concentrations of other elements increase during the first stage due to the dissolution of Ca. Most of the phases of BOF slag altered to compositionally heterogeneous V-containing iron, calcium, silicate hydrate phase (FCSH) or phases (Table 6). The chemical composition of the FCSH phase varied widely. The SiO_2 content varied from 17 to 28 wt%, the CaO content between 5 and 12 wt%, and the FeO content between 6 and 11 wt%. The V_2O_3 content remained high, varying between 3 and 6 wt%. Totals of the oxide analysis were rather small, at between 40 and 56 wt%, indicating there was a loose material structure containing a significant amount of hydroxyl water.

Differences in the reactivity of different phases and grain sizes were noted. The coarsest particles were only partially reacted, meaning they still containing the primary larnite, brownmillerite, and wüstite in the core areas. Moreover, tiny, seemingly unaltered brownmillerite and wüstite grains existed as inclusions in FCSH or associated with larnite in the bigger particles or as separate grains.

According to the EPMA–WDS and XRD results, Ca $(OH)_2$, $CaCO_3$, lime, and hatrurite, totally disappeared,

Table 5. Elemental concentrations of the residue from Ca leaching (L/S 5, 40°C, [NO_3^-] 7 mol/L, 20 min), as measured using ICP–OES.

Concentration of elements (mg/g)	Al	Ca	Fe	Mg	Mn	Si	V	Ti	P
Residue 1, after Ca leaching	11.40	158.70	201.10	13.10	28.50	73.90	31.00	8.6	5.56

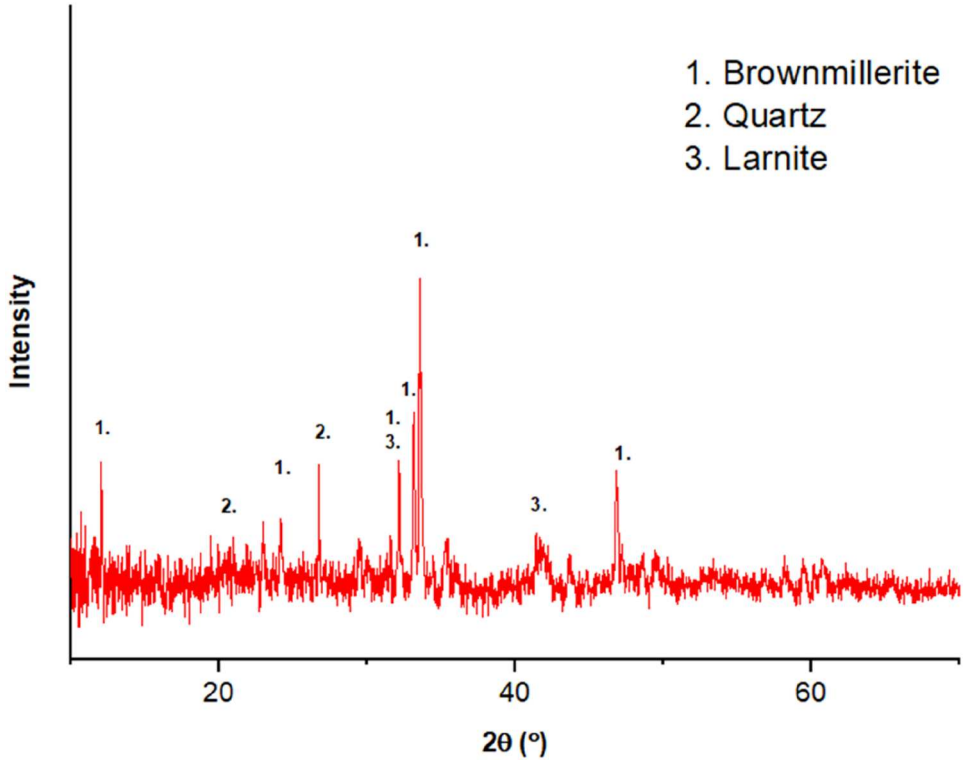

Figure 5. XRD analysis results for the residue after Ca leaching (7 mol/L, L/S ratio 5, 40°C, 20 min).

along with most of the larnite. However, according to FESEM (SD, Figure 2), some amount of CV remained after the Ca leaching stage. According to Table 6, the calcium ferrite was resistant to Ca leaching and contained about 17% of V content in the residue (SD, Figure 2). Based on these results, it can be inferred that Ca was essentially dissolved from lime, CV, calcium silicate phases, $CaCO_3$ and $Ca(OH)_2$. Most of the V (80-81%) was mainly in the formed FCSH phase (SD, Figure 2) but it is also likely that V may be present as ammonium vanadate in the residue. However, the presence of possible ammonium vanadate could not be detected with the methods used in this study.

3.5. Vanadium leaching

Ammonium salt leaching has been studied for the selective recovery of V. Precipitation of ammonium vanadate directly by cooling the solution has also been proposed as an advantage [15]. Ammonium salt leaching has been studied for roasted V slag [7,10,15]. However, the literature does not present the studies of V leaching with ammonium salt for steelmaking slag by direct leaching. In this study, ammonium salt leaching was investigated for the Ca-leached residue. Temperature, reaction time, [$(NH_4)_2CO_3$], L/S ratio, and repeating the leaching cycle were investigated to optimise V leaching efficiency and solution purity.

3.6. Effects of reaction time and temperature

In this study, the effect of temperature was studied together with the reaction time for the Ca-stage residue. The results are shown in Figure 6(a,b) and the measured elemental concentrations are presented in SD, Table 3.

It can be observed from Figure 6(a) that V dissolves already in 60 min with all studied temperatures. Its leaching efficiency changes only slightly when the reaction time is extended to 120 min. Based on this, it can be assumed that the dissolution of V proceeds rapidly. In many studies, it has been shown that in the

Table 6. EPMA–WDS analysis results for the residue after Ca leaching.

Phase	n	MgO	Al_2O_3	SiO_2	P_2O_5	Cr_2O_3	TiO_2	CaO	FeO	MnO	V_2O_3	Total
FCSH	9	0.20	1.16	21.46	1.46	0.20	0.71	8.07	8.94	1.70	4.55	48.45
Larnite	5	0.04	0.50	26.50	2.82	0.15	0.69	61.00	2.51	0.16	4.21	98.59
Ferrite	7	0.39	3.11	1.83	0.25	0.96	2.18	42.50	37.78	0.99	4.23	94.21
Wüstite	4	14.67	0.07	0.00	0.01	0.37	0.00	13.49	50.38	15.04	0.20	94.24

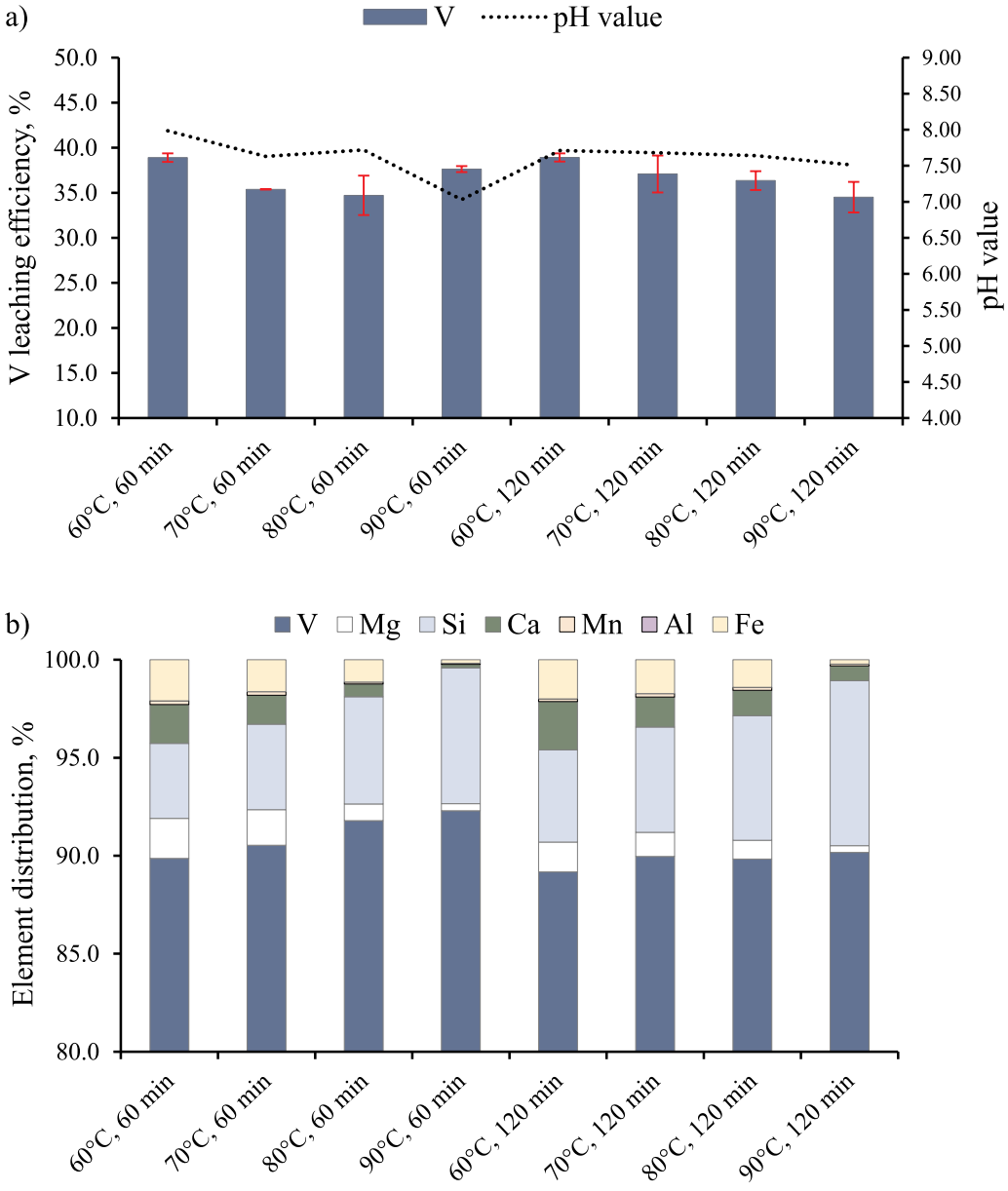

Figure 6. Effects of temperature and reaction time on (a) V recovery yield and (b) ED of the leachate (L/S ratio 8, concentration 100 g/L).

hydrometallurgical process of unroasted [21,41], and roasted slag [7,10,15], the leaching efficiency of V increases as a function of temperature. However, in this study increasing the temperature did not improve the leaching efficiency of V. It is unclear if the temperature and reaction time would affect the V-containing phases or whether the formed FCSH phase prevents the dissolution of V from the phases.

Temperature does not affect the total level of the impurities significantly over a longer reaction time (Figure 6(b)). The purity of the solution improves slightly when increasing the temperature with a shorter reaction time. Increasing the temperature significantly affects the Fe concentration with both reaction times. This may result from the oxidation of Fe, as supported by the lowering pH as the temperature increases and the Fe

concentration decreases (Equations 6 and 7).

$$Fe^{2+}(aq) \rightarrow Fe^{3+}(aq) + e^{-} \quad (6)$$

$$Fe^{3+}(aq) + 3H_2O\ (l) \rightarrow Fe(OH)_3(s) + 3H^{+}(aq) \quad (7)$$

Ca and Mg concentrations reduce when the temperature is increased (Mg 1.9–0.3%, Ca 2.4–0.2%). In the presence of carbonate ions, Ca and Mg ions precipitate as insoluble calcium and magnesium carbonates ($CaCO_3$ and $MgCO_3$) (Equations 8 and 9). This probably affects the decrease in pH.

$$(NH_4)_2CO_3\ (s) + H_2O\ (l) \rightarrow 2NH_4^{+}\ (aq) + HCO_3^{-}\ (aq) + OH^{-}\ (aq) \quad (8)$$

$$2HCO_3^{-}\ (aq) + 2OH^{-}\ (aq) + Mg^{2+}(aq) + Ca^{2+}(aq) \rightarrow CaCO_3(s) + MgCO_3(s) + 2H_2O\ (l) \quad (9)$$

It also can be seen from Figure 6(b) that increasing the temperature dramatically increases the Si concentration n the leachate (from 3.8–6.9%). Preventing the dissolution of Si is important for ensuring the simplicity of the process and the recycling of leachate. However, the precipitated product may contain impurities as shown above (MgCO3, $CaCO_3$ e.g.). Some of these can possibly be washed from the precipitated product with an acidic ammonium salt solution, such as NH_4NO_3. Furthermore, too high temperature can decompose ammonium carbonate into carbon dioxide and ammonia. Therefore, a temperature of 60°C and reaction time of 60 min were selected for the following experiments.

3.7. Effects of L/S ratio, $[(NH_4)_2CO_3]$, and repeating leaching cycle

The effect of the L/S ratio on the V leaching efficiency was investigated. It can be seen from Figure 7(a) that increasing the L/S ratio improved slightly the dissolution of V. The literature reveals that this action improves the V leaching rate also in alkaline leaching of unroasted slag [41], ammonium salt leaching [15] and ammonium salt–acid leaching [8] of roasted slag. In the present study, increasing the L/S ratio also increased the concentrations of impurities such as Fe, Mg, Ca, Si. This can be seen in Figure 7(b) (elemental concentrations in SD, Table 4). Based on the results, L/S ratio 8 was selected to the further experiments.

Several studies have been presented in the literature, where increasing the concentration of the leaching reagent, increases V leaching efficiency from roasted slag [7,15]. The results of this study partly agree with them. However, it should be noted that the results cannot be directly compared to the literature research due to the absence of a roasting stage. The investigated $[(NH_4)_2CO_3]$ range was 100–600 g/L (60 °C, 8 mL/g) and the effect for the V leaching efficiency and the ED in the leachate is shown in Figure 8(a,b).

Figure 8(a) shows that $[(NH_4)_2CO_3]$ had the predominant effect on the leaching efficiency of V. Increasing the concentration to 200 g/L improved the V leaching efficiency to 50%. After this, increasing the concentration decreased the leaching efficiency of V. This may be due either to a large excess of ammonium relative to the V concentration [42], or a secondary phase to have formed that could prevent leaching.

The purity of the leachate remained at a high level while the concentration was increased up to 200 g/L (Figure 8(b)) but started to decrease slightly at a concentration of 300 g/L. Measured concentrations are presented in SD, Table 5. The concentrations of the impurities increased significantly when $[(NH_4)_2CO_3]$ was 400 g/L or greater. The main impurity in the leachate was Fe. Its concentration was under 20 ppm (pH 9.09) in the optimised condition. [Fe] increased to 709 ppm when $[(NH_4)_2CO_3]$ was 400 g/L, and it increased further to 2575 ppm with 600 g/L $[(NH_4)_2CO_3]$. The highest concentration corresponded to about 18% of the Fe content in the solid residue. The results for the Fe dissolution is difficult to explain based on the leaching conditions (pH 9.49–9.69). Therefore, it remains unclear which mechanism affects Fe leaching. Further research should focus on this mechanism and higher $[(NH_4)_2CO_3]$, studying the effects of different reaction conditions on the leaching efficiency of V.

The repeating of the leaching cycle was studied with optimised conditions. After the first leaching (60 min, 60 °C, 200 g/L $[(NH_4)_2CO_3]$, L/S ratio 8), the residue was washed and dried. A second leaching round was performed with a new portion of the leaching solution, in the same reaction conditions as the first leaching round. The results can be seen in Figure 9.

It was possible to dissolve 21% of the remaining amount of V during the second leaching cycle. This increased the total leaching efficiency to 60.7% but at the same time increased the concentrations of impurities significantly. This was expected as the reaction conditions were not optimised, and the amount of V was greatly lowered in the residue after the first round. This experiment demonstrated the possibility of improving the V leaching efficiency by reprocessing the residue. However, if this step was to be utilised to improve V leaching efficiency, it would require optimisation to achieve higher solution purity.

3.8. Characterization of residue

After the second stage, the concentrations of the elements in the residue were analysed using microwave-assisted

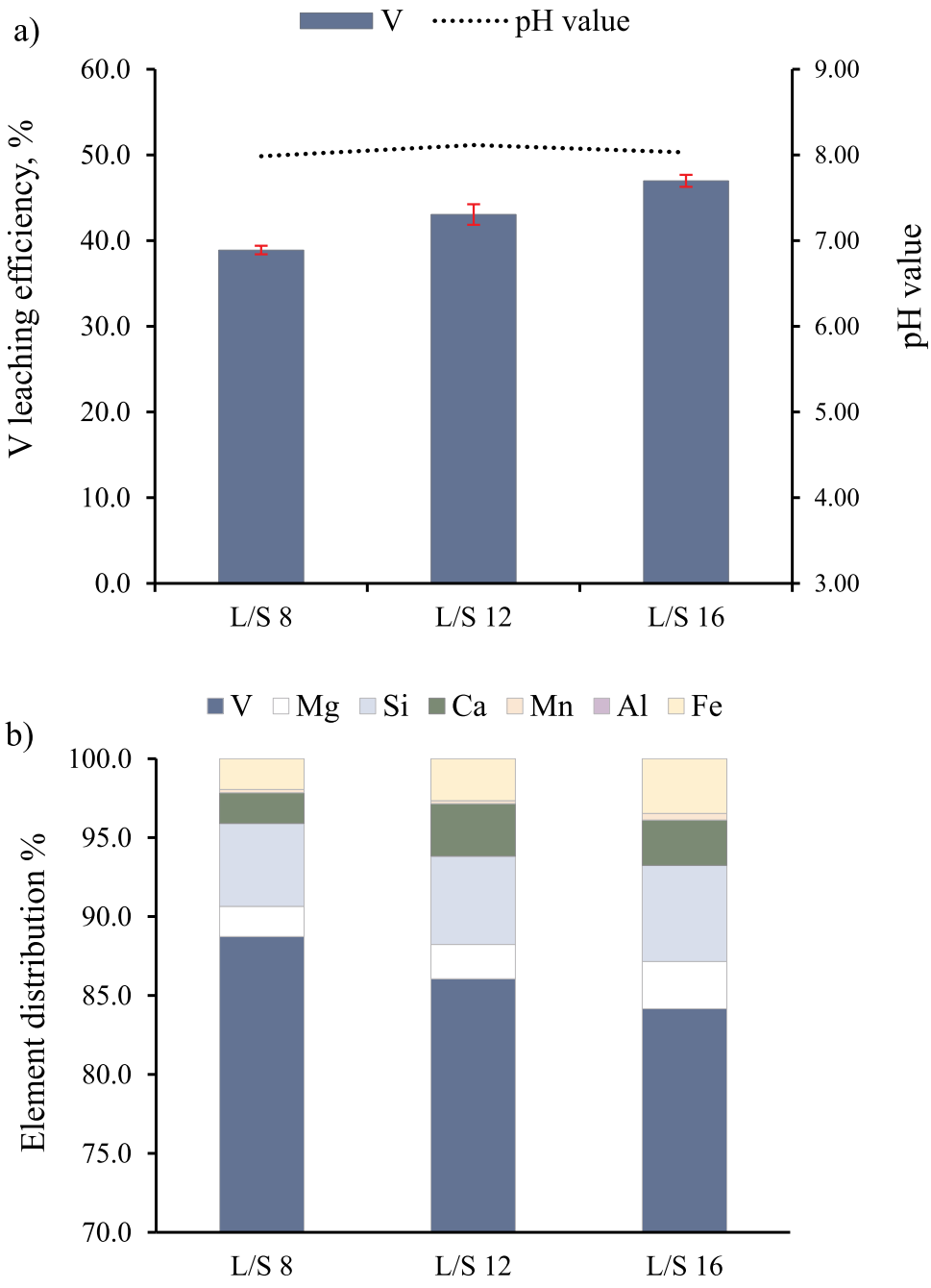

Figure 7. Effects of the L/S ratio on the (a) V leaching efficiency and (b) ED of the leachate (60 min, 60°C, 100 g/L $(NH_4)_2CO_3$).

acid digestion and ICP–OES (Table 7). The phase composition was analysed using EPMA–WDS (Table 8).

Table 7 shows that V leached while the other elements were mainly enriched in the residue. The microstructural appearance of the residue was not much changed compared to the Ca-stage residue. The coarsest particles still contained the primary minerals larnite, calcium ferrite, and wüstite in the core areas. Based on the EPMA–WDS results, most of the material was compositionally heterogenous FCSH phase where SiO_2 content varied from 16 to 29 wt%, and CaO from 2 to 19 wt%. FeO content was between 9 and 11 wt%, and V_2O_3 between 1 and 3 wt%. Totals of the oxide analysis were small, at between 41 and 62 wt%, indicating that material structure contained a large amount of hydroxyl water.

It seems that V had dissolved from the FCSH phase due to a lowered V content (Table 8). FESEM-EDS reveals that V has probably also dissolved from CV, as the phase has disappeared during V leaching stage (SD, Figure 3). Unreacted ferrite and intact but scarce larnite still contained V (Table 8).

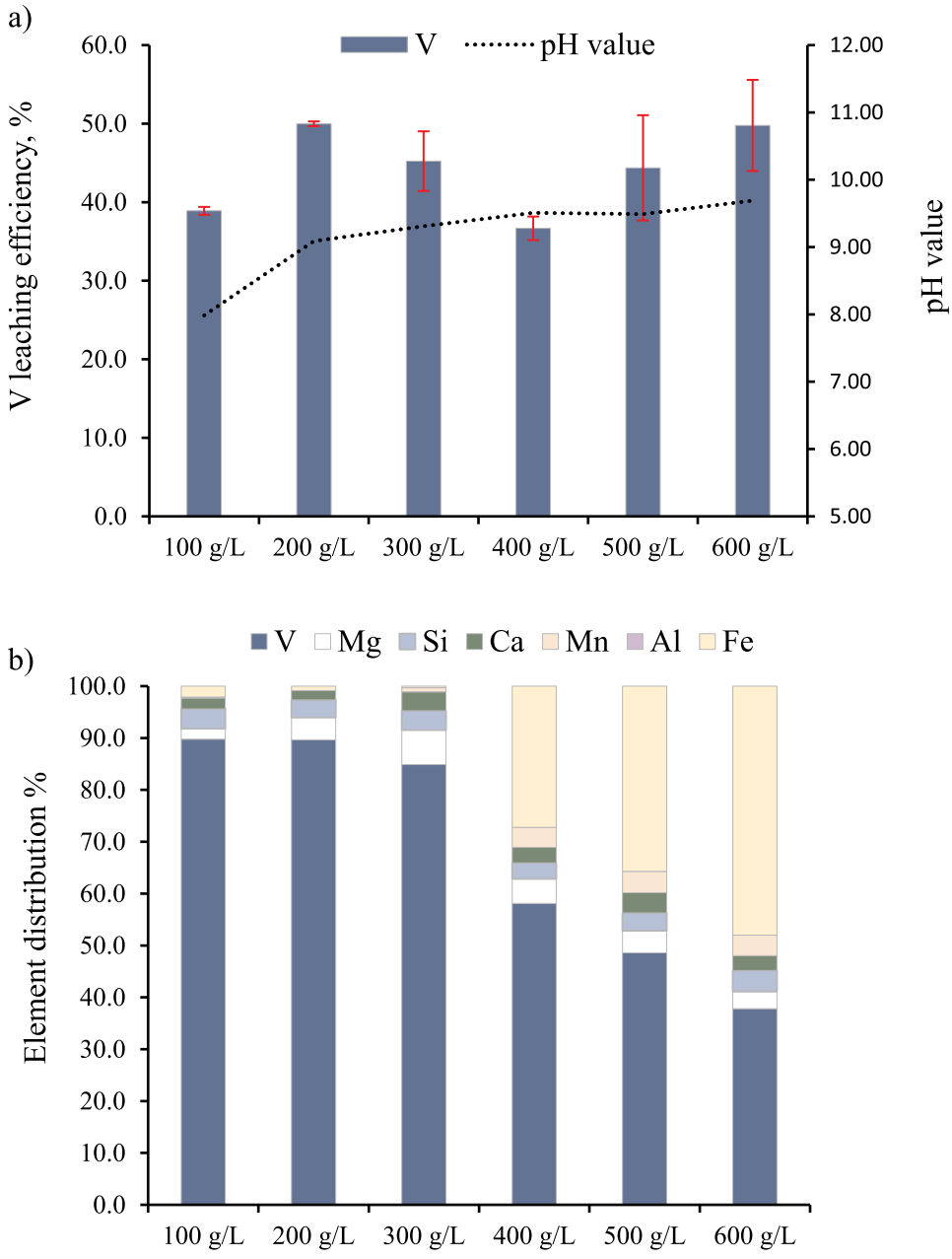

Figure 8. Effect of [$(NH_4)_2CO_3$] on the (a) V leaching efficiency and (b) ED in the leachate (60 min, 60°C, and L/S 8).

Based on the EPMA–WDS analyses (Tables 6 and 8), Ca content decreased in the FCSH phase during the V-stage. According to the ICP–OES results Ca was not released into the solution. This indicates that Ca was precipitated as $CaCO_3$. Ca–Mg carbonate phase was observed in the XRD analysis of the V-stage residue (Figure 10) and also with FESEM-EDS. DSC-TG-MS analysis (Figure 11(a,b)) supported this result. The first DSC peak, with a temperature of about 100°C, was caused by rapid H_2O (m/z 18) removal. Another 4% weight loss took place in the period until the temperature reached 650°C. The second DSC peak with a temperature of 670–720°C, could have been associated with CO_2 (m/z 44) removal, and the total corresponded with a weight loss of 14%. The peak at 670–720°C further suggested the presence of carbonate compounds in the residue.

4. Conclusions

To achieve a more comprehensive utilisation process for high-Ca content BOF slag a direct two-stage leaching process of Ca and V was proposed. This method provides a higher utilisation rate of slag due to Ca recovery. In the first stage, Ca is leached selectively, and the leachate can be directed to the PCC process where sulfate-free side

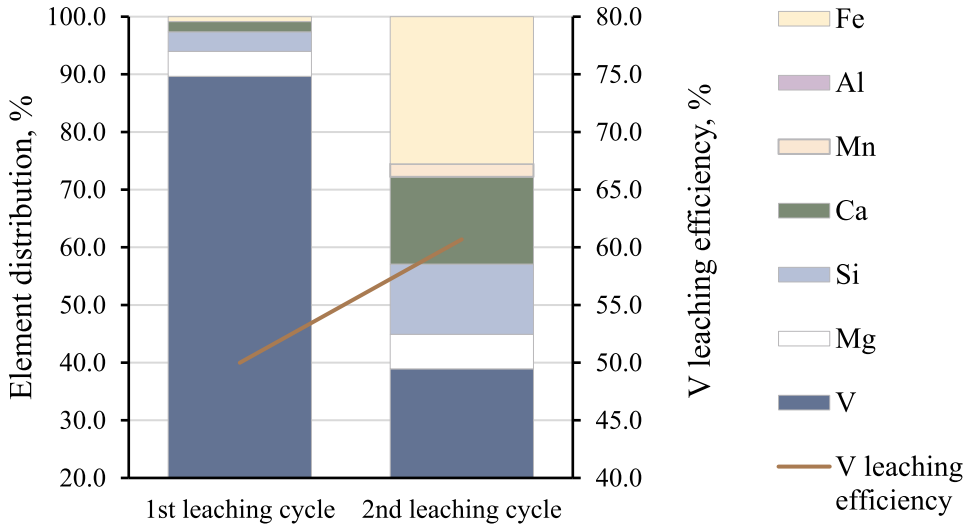

Figure 9. Effect of second leaching cycle on ED of the leachate and V leaching efficiency.

Table 7. Elemental concentrations of V leaching residue as measured using ICP–OES.

Concentration of elements (mg/g)	Al	Ca	Fe	Mg	Mn	Si	V	Ti	P
Residue 2, after V leaching	11.10	161.50	190.80	12.10	27.20	73.80	16.90	7.88	5.04

Table 8. EPMA–WDS analysis results for the residue after the V-stage.

Phase	n	MgO	Al_2O_3	SiO_2	CaO	FeO	MnO	TiO_2	P_2O_5	Cr_2O_3	V_2O_3	Total
FCSH	17	0.49	1.44	23.19	6.23	12.39	1.35	0.87	1.19	0.19	2.16	49.49
Larnite	6	0.00	0.60	26.45	62.42	1.50	0.06	0.69	2.89	0.12	4.47	99.19
Ferrite	4	0.55	6.50	0.60	43.16	29.26	0.71	4.37	0.07	1.26	7.11	93.59
Wüstite	13	7.06	0.09	0.00	11.96	59.99	14.44	0.05	0.01	0.22	0.26	94.07

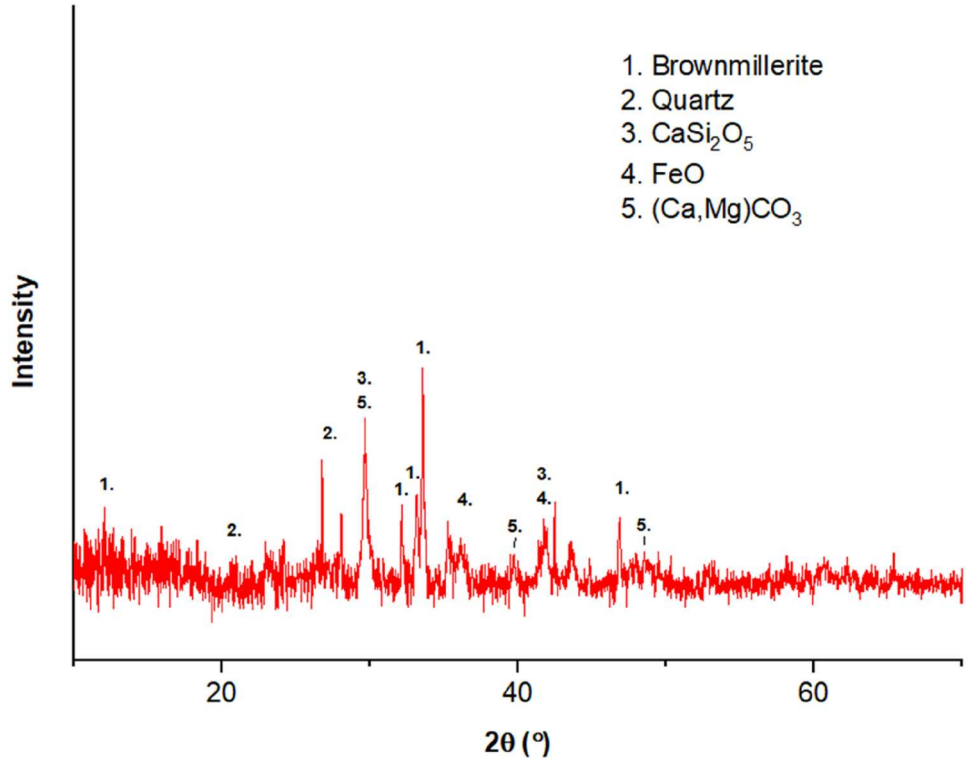

Figure 10. XRD ratio 8, ($(NH_4)_2CO_3$ 300 g/L). analysis results of residue from V leaching (60°C, 60 min, L/S 8).

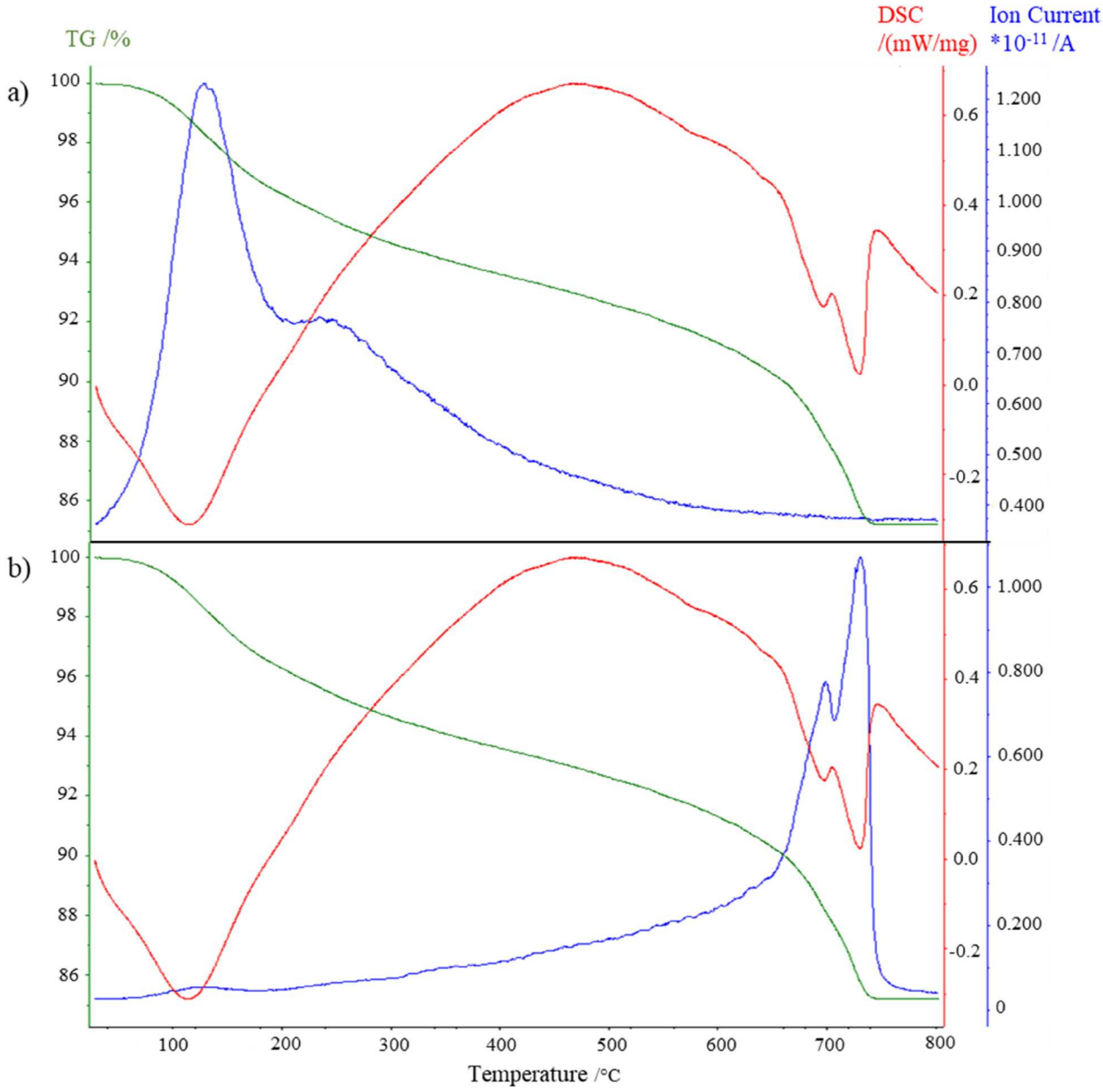

Figure 11. Thermal decomposition curves for V-stage residue: (a) fragment m/z 18 (H_2O^+), (b) fragment m/z 44 (CO_2^+). Green curve = TG, blue curve = MS(MID), red curve = DSC.

product ($CaCO_3$) can be produced. The PCC process sequesters significant amounts of carbon dioxide (CO_2). The residue from the Ca-stage is directed to the second leaching stage, from which V can be recovered as ammonium vanadate.

In the first stage, the formed solution contained more than 99% Ca of all dissolved elements. V loss was minor in this stage. Ca leaching efficiency was 71.1% with the L/S ratio 5, temperature 40 °C, reaction time 20 min, and [NO_3^-] 7 mol/L (NH_4NO_3/HNO_3 ratio 3:1). Residue from the first stage was directed to the second leaching stage where V leaching was performed by ammonium salt solution. The V leaching efficiency was 50.0%, and V was more than 88% of all dissolved elements. These results were obtained at the temperature 60 °C, L/S ratio 8, reaction time 60 min, and [$((NH_4)_2CO_3)$] 200 g/L. Based on comprehensive mineralogical analyses, it was observed that in the residue after Ca leaching V occurs mainly in the formed FCSH phase and calcium ferrite, with minor amounts in the CV and larnite relicts, although a significant amount of larnite was affected by Ca leaching. The FCSH phase was largely formed during Ca leaching stage from the phases (silicates, CV, CaO, $Ca(OH)_2$, $CaCO_3$) from which Ca was dissolved.

Formation of the FCSH and the perseverance of calcium ferrites throughout both leaching likely hinder the possibility to achieve higher V leaching efficiency and selectivity under studied reaction conditions.

The significant advantages of this method are related to environmental and energy aspects due to the low temperatures in leaching treatments and without a roasting stage. The utilisation rate of side streams with a low V content can be increased by recovering Ca as well. Furthermore, the leachates from both leaching stages can be cycled back into the processes, thus significantly reducing the amount of wastewater. However, further optimisation and developments are required regarding the effectiveness of the process, especially to improve the selectivity of the V leaching stage and V leaching efficiency from both FCSH and calcium ferrite.

Acknowledgments

The authors would like to thank Mr. Tommi Kokkonen (Unit of Process Metallurgy) for the DSC-TG-MS analysis, Mr. Jarno Karvonen (Unit of Fibre and Particle Engineering) for the grinding, and Mr. Markus Väyrynen (Unit of Sustainable Chemistry) for the ICP–OES analyses.

Disclosure statement

No potential conflict of interest was reported by the author(s).

Funding

This work was funded by Business Finland through High-Potential Inorganic Side Streams project (MIMEPRO; No. 7935/31/2019), and Towards Carbon-Neutral Metals project (TOCANEM; No. 41700/31/2020).

Data availability statement

The data of this study is available upon reasonable request.

ORCID

Janne Pesonen http://orcid.org/0000-0001-8851-5460

References

[1] D.-G. for I. M. I. E. and Sme. European Commission. COMMUNICATION FROM THE COMMISSION TO THE EUROPEAN PARLIAMENT, THE COUNCIL, THE EUROPEAN ECONOMIC AND SOCIAL COMMITTEE AND THE COMMITTEE OF THE REGIONS Critical Raw Materials Resilience: Charting a Path towards greater Security and Sustainability. Brussels, 2020. Accessed: May 06, 2022. [Online]. Available: https://eur-lex.europa.eu/legal-content/EN/TXT/?uri=CELEX%3A52020DC0474&qid=1651831561005

[2] Moskalyk RR, Alfantazi AM. Processing of vanadium: a review. Miner Eng. 2003;16(9):793–805. doi: 10.1016/S0892-6875(03)00213-9

[3] Wu K, Wang Y, Wang X, et al. Co-extraction of vanadium and chromium from high chromium containing vanadium slag by low-pressure liquid phase oxidation method. J Clean Prod. 2018;203:873–884. doi: 10.1016/j.jclepro.2018.08.288

[4] Liu S, Ding E, Ning P, et al. Vanadium extraction from roasted vanadium-bearing steel slag via pressure acid leaching. J Environ Chem Eng. 2021;9(3). doi: 10.1016/j.jece.2021.105195

[5] Kawatra SK, Young C. Sme mineral processing and extractive metallurgy handbook. Englewood, CO: Society for Mining, Metallurgy, and Exploration, Inc; 2019. [Online]. Available: http://pc124152.oulu.fi:8080/login?url=

[6] Swinbourne DR, Richardson T, Cabalteja F. Understanding ferrovanadium smelting through computational thermodynamics modelling. Min Proc Extractive Metall. 2016;125(1):45–55. doi: 10.1179/1743285515Y.0000000019

[7] Li M, Liu B, Zheng S, et al. A cleaner vanadium extraction method featuring non-salt roasting and ammonium bicarbonate leaching. J Clean Prod. 2017;149:206–217. doi: 10.1016/j.jclepro.2017.02.093

[8] Wen J, Jiang T, Zhou W, et al. A cleaner and efficient process for extraction of vanadium from high chromium vanadium slag: leaching in (NH4)2SO4-H2SO4 synergistic system and NH4+ recycle. Sep Purif Technol. 2019;216:126–135. doi: 10.1016/j.seppur.2019.01.078.

[9] Li X, Xie B. Extraction of vanadium from high calcium vanadium slag using direct roasting and soda leaching. Int J Min Metall Mat. 2012;19:595–601. doi: 10.1007/s12613-012-0600-8

[10] Li M, et al. Extraction of vanadium from vanadium slag via Non-salt roasting and ammonium oxalate Leaching. JOM. 2017;69(10):1970–1975. doi: 10.1007/s11837-017-2494-4

[11] Aarabi-Karasgani M, Rashchi F, Mostoufi N, et al. Leaching of vanadium from LD converter slag using sulfuric acid. Hydrometallurgy. 2010;102(1–4):14–21. doi: 10.1016/j.hydromet.2010.01.006

[12] Yang Z, Li H-Y, Yin X-C, et al. Leaching kinetics of calcification roasted vanadium slag with high CaO content by sulfuric acid. Int J Miner Process. 2014;133:105–111. doi: 10.1016/j.minpro.2014.10.011

[13] Wen J, Jiang T, Zhou M, et al. Roasting and leaching behaviors of vanadium and chromium in calcification roasting–acid leaching of high-chromium vanadium slag. Int J Min Metall Mat. 2018;25(5):515–526. doi: 10.1007/s12613-018-1598-3

[14] Wen J, Jiang T, Arken S. Selective leaching of vanadium from vanadium-chromium slag using sodium bicarbonate solution and subsequent in-situ preparation of flower-like VS2. Hydrometallurgy. 2020;198:105498. doi: 10.1016/j.hydromet.2020.105498.

[15] Li H-Y, Wang K, Hua W-H, et al. Selective leaching of vanadium in calcification-roasted vanadium slag by ammonium carbonate. Hydrometallurgy. 2016;160:18–25. doi: 10.1016/j.hydromet.2015.11.014

[16] Li H-Y, Fang HX, Wang X, et al. Asynchronous extraction of vanadium and chromium from vanadium slag by stepwise sodium roasting-water leaching. Hydrometallurgy. 2015;156:124–135. doi: 10.1016/j.hydromet.2015.06.003

[17] Mirazimi SMJ, Rashchi F, Saba M. A new approach for direct leaching of vanadium from LD converter slag. Chem Eng Res Des. 2015;94:131–140. doi: 10.1016/j.cherd.2014.12.010

[18] Liu L, Kauppinen T, Tynjälä P, et al. Water leaching of roasted vanadium slag: Desiliconization and precipitation of ammonium vanadate from vanadium solution. Hydrometallurgy. 2023;215; doi: 10.1016/j.hydromet.2022.105989

[19] Wen J, Jiang T, Liu Y, et al. Extraction behavior of vanadium and chromium by calcification roasting-acid leaching from high chromium vanadium slag: optimization using response surface methodology. Miner Process Extr Metall Rev. 2019;40(1):56–66. doi: 10.1080/08827508.2018.1481059

[20] Xiong P, Zhang Y, Bao S, et al. Precipitation of vanadium using ammonium salt in alkaline and acidic media and the effect of sodium and phosphorus. Hydrometallurgy. 2018;180:113–120. doi: 10.1016/j.hydromet.2018.07.014

[21] Peng H, Liu Z, Tao C. Leaching kinetics of vanadium with electro-oxidation and H_2O_2 in alkaline medium Energy Fuels. 2016;30(9):7802–7807. doi: 10.1021/acs.energyfuels.6b01364

[22] Hu K, Liu X, Liu Q. Extracting vanadium from stone coal by a cyclic alkaline leaching method. Metall Mater Trans B. 2017;48(2):1342–1347. doi: 10.1007/s11663-016-0906-4

[23] Mombelli D, Mapelli C, Barella S, et al. The effect of chemical composition on the leaching behaviour of electric arc furnace (EAF) carbon steel slag during a standard leaching test. J Environ Chem Eng. 2016;4:1050–1060. doi: 10.1016/j.jece.2015.09.018

[24] Li Y, Meng X, Chen K, et al. Crystallization behaviors of spinel during cooling process of modified EAF slag. Metall Mater Trans B. 2020;51(3):1027–1038. doi: 10.1007/s11663-020-01802-2

[25] Said A, Mattila O, Eloneva S, et al. Enhancement of calcium dissolution from steel slag by ultrasound. Process Intensif. 2015;89:1–8. doi: 10.1016/j.cep.2014.12.008

[26] Ragipani R, Bhattacharya S, Akkihebbal SK. Understanding dissolution characteristics of steel slag for resource recovery. Waste Manage. 2020;117:179–187. doi: 10.1016/j.wasman.2020.08.008.

[27] Mei X, Zhao Q, Min Y, et al. Phase transition and dissolution behavior of Ca/Mg-bearing silicates of steel slag in acidic solutions for integration with carbon sequestration. Process Saf Environ Prot. 2022;159:221–231. doi: 10.1016/j.psep.2021.12.062.

[28] Navarro R, Guzman J, Saucedo I, et al. Vanadium recovery from oil fly ash by leaching, precipitation and solvent extraction processes. Waste Manage. 2007;27(3):425–438. doi: 10.1016/j.wasman.2006.02.002

[29] Muthukumar K, Patel KM, Mohapatra D, et al. Selective recovery of vanadium as AMV from calcium vanadate sludge by direct AS leaching process: an industrial approach. Waste Manage. 2020;102:815–822. doi: 10.1016/j.wasman.2019.11.040

[30] Wunderlich S, Schirmer T, Fittschen UEA. Investigation on vanadium chemistry in basic-oxygen-furnace (BOF) slags—A first approach. Metals (Basel). 2021;11(11):1869. doi: 10.3390/met11111869

[31] Eloneva S, Teir S, Revitzer H, et al. Reduction of CO2 Emissions from steel plants by using steelmaking slags for production of marketable calcium carbonate. Steel Res Int. 2009;80(6):415–421. doi: 10.2374/SRI09SP028

[32] Rantala V, et al. Elemental concentrations of natural graphite and steelmaking slag: development of microwave-assisted acid digestion. Anal Lett. 2023: 1–16. doi: 10.1080/00032719.2023.2289083

[33] Hu X, Yue Y, Peng X. Release kinetics of vanadium from vanadium (III, IV and V) oxides: effect of pH, temperature and oxide dose. J Environ Sci. 2018;67:96–103. doi: 10.1016/j.jes.2017.08.006

[34] Eloneva S, Said A, Fogelholm C-J, et al. Preliminary assessment of a method utilizing carbon dioxide and steelmaking slags to produce precipitated calcium carbonate. Appl Energy. 2012;90(1):329–334. doi: 10.1016/j.apenergy.2011.05.045.

[35] Yang B, He J, Zhang G, et al., eds. Vanadium and its compounds. In: Vanadium. Extraction, manufacturing, and applications. Elsevier; 2021. p. 9–32. doi: 10.1016/B978-0-12-818898-9.00002-4

[36] Eloneva S, Teir S, Salminen J, et al. Steel converter slag as a raw material for precipitation of pure calcium carbonate. Ind Eng Chem Res. 2008;47(18):7104–7111. doi: 10.1021/ie8004034

[37] Owais M, Järvinen M, Taskinen P, et al. Experimental study on the extraction of calcium, magnesium, vanadium and silicon from steelmaking slags for improved mineral carbonation of CO2. J CO2 Utiliz. 2019;31:1–7. doi: 10.1016/j.jcou.2019.02.014

[38] Seggiani M., Vitolo S. Recovery of silica gel from blast furnace slag. Resour Conserv Recycl. 2003;40(1):71–80. doi: 10.1016/S0921-3449(03)00034-X

[39] Song K, Park S, Kim W, et al. 'Effects of experimental parameters on the extraction of silica and carbonation of blast furnace slag at atmospheric pressure in low-concentration acetic acid'. Metals (Basel). 2017;7(6):199. doi: 10.3390/met7060199

[40] Peng H. A literature review on leaching and recovery of vanadium. J Environ Chem Eng. 2019;7(5):103313. doi: 10.1016/j.jece.2019.103313

[41] Wan J, Du H, Gao F, et al. Direct leaching of vanadium from vanadium-bearing steel slag using NaOH solutions: a case study. Miner Process Extr Metall Rev. 2021;42(4):257–267. doi: 10.1080/08827508.2020.1762182

[42] Wen J, Jiang T, Xu Y, et al. Efficient extraction and separation of vanadium and chromium in high chromium vanadium slag by sodium salt roasting-(NH4)2SO4 leaching. J Ind Eng Chem. 2019;71:327–335. doi: 10.1016/j.jiec.2018.11.043